ACS chemical biology

Articles

pubs.acs.org/acschemicalbiology

Estrogen Receptor Folding Modulates cSrc Kinase SH2 Interaction via a Helical Binding Mode

Lidia Nieto,[†,§] Inga M. Tharun,[†,§] Mark Balk,[†] Hans Wienk,[‡] Rolf Boelens,[‡] Christian Ottmann,[†] Lech-Gustav Milroy,[†] and Luc Brunsveld*[,†]

[†]Laboratory of Chemical Biology, Department of Biomedical Engineering and Institute of Complex Molecular Systems, Eindhoven University of Technology, 5612AZ Eindhoven, The Netherlands

[‡]Bijvoet Center for Biomolecular Research, NMR Spectroscopy Utrecht University, 3584CH Utrecht, The Netherlands

Supporting Information

ABSTRACT: The estrogen receptors (ERs) feature, next to their transcriptional role, important nongenomic signaling actions, with emerging clinical relevance. The Src Homology 2 (SH2) domain mediated interaction between cSrc kinase and ER plays a key role in this; however the molecular determinants of this interaction have not been elucidated. Here, we used phosphorylated ER peptide and semisynthetic protein constructs in a combined biochemical and structural study to, for the first time, provide a quantitative and structural characterization of the cSrc SH2−ER interaction. Fluorescence polarization experiments delineated the SH2 binding motif in the ER sequence. Chemical shift perturbation analysis by nuclear magnetic resonance (NMR) together with molecular dynamics (MD) simulations allowed us to put forward a 3D model of the ER-SH2 interaction. The structural basis of this protein−protein interaction has been compared with that of the high affinity SH2 binding sequence GpYEEI. The ER features a different binding mode from that of the "two-pronged plug two-hole socket" model in the so-called specificity determining region. This alternative binding mode is modulated via the folding of ER helix 12, a structural element directly C-terminal of the key phosphorylated tyrosine. The present findings provide novel molecular entries for understanding nongenomic ER signaling and targeting the corresponding disease states.

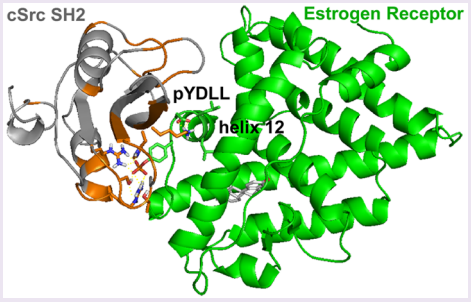

The estrogen receptors (ERs) α and β are members of the nuclear receptor transcription factor family. They are typically characterized as ligand-activated transcription factors that control gene expression by direct binding to estrogen ligands such as the endogenous estradiol, E2.[1] The C-terminal activation function 2 (AF2) of the ER, comprising the most C-terminal regulatory helix 12 (H12) of the ER ligand binding domain (LBD), is of central importance in the control of this activation mechanism.[2,3] Transcriptional regulation is additionally controlled by various other mechanisms such as interacting coregulator proteins[4,5] and post-translational modifications (PTMs).[6−8] For instance, recent studies on the phosphorylation of tyrosines (Y) Y537 and Y488, in the ERα and ERβ LBDs, respectively, have shown a subtype-specific modulation of ER-coactivator interaction by phosphorylation.[9] Next to this classical genomic mechanism, the ER also plays an important role in various rapid signaling pathways by nongenomic mechanisms, including the Ras/Raf/MAPK, p38/MAPK, PI3K/AKT, PLC/PKC, and cAMP/PKA pathways.[10−13] ER can activate the MAPK pathway by binding to several signaling proteins simultaneously, such as to the cSrc kinase and to MNAR, the modulator of nongenomic activity of ER.[14,15] This protein interplay results in the activation of the cSrc/MAPK-pathway, which subsequently leads to ERα phosphorylation on S118 and thereby enhanced ERα transcriptional activity. It has also been reported that agonistic steroid ligands induce the formation of a complex between ER, the androgen receptor (AR), and the cSrc kinase.[16] This ternary complex results in downstream modulation of the cSrc/Raf-1/Erks-pathway.[15,16] In these nongenomic actions of ER, PTMs play a key role in regulating the function of the receptor. The interaction between ER and the phosphotyrosine-interacting SH2 domain of cSrc kinase has been proposed to depend on the phosphorylation state of AF2—more specifically of Y537 and Y488, in ERα and ERβ, respectively.[16−18] In line with this, mutations of these phosphorylatable residues as well as mutations in their direct vicinity significantly modify the receptors' activity.[19−22] Interestingly, the aforementioned tyrosine Y537 has been demonstrated to be a hotspot for mutations in ER in hormone-resistant metastatic breast cancer.[23−28] These findings, together with the fact that elevated expression levels of cSrc kinase have been reported in cancer cells,[29−31] show the clinical relevance of these protein−protein interactions.[32−34]

Studies into the nontranscriptional functions of ER have been limited to cellular work. The temporal character of PTMs in the cellular setting and the absence of techniques to provide structural information in cells have prevented the molecular

Received: July 21, 2015
Accepted: September 9, 2015
Published: September 9, 2015

DOI: 10.1021/acschembio.5b00568
ACS Chem. Biol. 2015, 10, 2624−2632

Table 1. Peptide Sequences of FAM-labeled Phosphorylated and Nonphosphorylated ER Peptides and Proteins and Their K_D Values (in μM) As Determined by a Direct FP Binding Assay in the Titration with vSrc and cSrc Kinase SH2 Domains

peptide number	peptide/protein[a]	sequence	cSrc SH2 K_d (μM)	vSrc SH2 K_d (μM)
1	ERα 21-mer	$_{530}$CKNVVPLYDLLLEMLDAHRLK$_{550}$-(FAM)	n.b.[b]	n.b.
2	pERα 21-mer	$_{530}$CKNVVPLpYDLLLEMLDAHRLK$_{550}$-(FAM)	11 ± 0.6	4.2 ± 0.2
3	ERβ 21-mer	$_{481}$CKNVVPVYDLLLEMLNAHVLK$_{501}$-(FAM)	n.b.	n.b.
4	pERβ 21-mer	$_{481}$CKNVVPVpYDLLLEMLNAHVLK$_{501}$-(FAM)	8.5 ± 0.5	5.7 ± 0.4
5	hmT antigen 5-mer	(FAM)-$_{323}$GYEEI$_{327}$	n.b.	n.b.
6	phmT antigen 5-mer	(FAM)-$_{323}$GpYEEI$_{327}$	0.45 ± 0.03	0.98 ± 0.05
	ERβ LBD	ERβ LBD (L260-K501)-FAM	n.b.	n.b.
	pERβ LBD	ERβ LBD (L260-pTyr488-K501)-FAM[9]	12 ± 4	n.d.[c]

[a]ER = estrogen receptor. *p* = phosphorylated. hmT antigen = hamster polyomavirus middle size tumor antigen. [b]n.b. = no binding. [c]n.d. = not determined.

characterization of these interactions. As such, the exact molecular determinants of this interaction are not known and require elucidation to provide novel molecular entries for understanding the resulting signaling and targeting the corresponding disease states. In this work, we combined biochemical and NMR techniques to study the interaction between phosphorylated segments of the ERα and ERβ subtypes and the cSrc kinase SH2 domain. Peptide constructs were studied to delineate the SH2 binding motif in the ER sequences. The complete and phosphorylated ER LBD, obtained via a protein semisynthesis approach,[9,35,36] was used to obtain the first molecular characterization of the interaction between an entire ER LBD and the cSrc kinase SH2 domain. The structural basis of this protein−protein interaction has been compared with that of the high affinity SH2 binding sequence GpYEEI,[37] finding a different binding mode to that of the "two-pronged plug two-hole socket" model in the so-called specificity determining region. The present findings provide the first molecular insights on how ER interacts with cSrc and how ER PTMs control nuclear receptor nongenomic signaling in synergy with protein folding.

RESULTS AND DISCUSSION

Molecular Determinants of ER−SH2 Interaction. A set of relatively long peptide sequences (21 amino acids length), were prepared to evaluate the binding characteristics to Src SH2 domains. The peptides were designed to feature substantial amino acids flanking the tyrosines of interest of both ER subtype sequences and were synthesized in their phosphorylated (pERα/pERβ) and nonphosphorylated state and featuring a C-terminal incorporated fluorescent label (Table 1, **1**−**4**). A fluorescence polarization (FP) binding assay was performed to determine the binding affinities of these ER peptides to the cSrc SH2 as well as to its viral homologue vSrc SH2 domain (97% identical in sequence), for reference. Also the binding of the full length, tyrosine phosphorylated, and C-terminal fluorescently labeled ERβ LBD[9] to cSrc SH2 was studied. Serial dilutions of the SH2 protein were titrated to constant concentrations of the peptide or protein (Table 1, Figures 1A and S5). For comparison, a high affinity binding sequence (GpYEEI) derived from the hamster polyomavirus middle size tumor antigen and its nonphosphorylated homologue were studied (Table 1, **5** and **6**, Figure 1B). For all constructs, tyrosine phosphorylation turned out to be an absolute necessity for the interaction with SH2. This is in line with the described switch function of tyrosine phosphorylation for the Src SH2 interaction with its cognate proteins.[38] Binding to the phosphorylated ER sequences revealed similar affinities

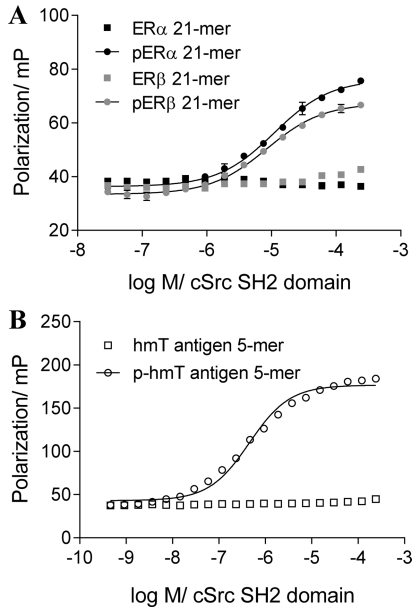

Figure 1. Fluorescence polarization assay (A). Titration of cSrc SH2 domain to FAM-labeled phosphorylated ('p', circles) and non-phosphorylated (squares) ERα (black) and ERβ (gray) H12 peptides (corresponding to peptides **1**−**4** in Table 1). For comparison (B): Titrations of the phosphorylated (circles) and nonphosphorylated (squares) FAM-labeled high affinity binding motif hmT antigen 5-mer peptides (corresponding to peptides **5** and **6** in Table 1) with the cSrc kinase SH2 domain. The titrations with the vSrc kinase SH2 domain and of the full length phosphorylated ERβ LBD can be found in the Supporting Information (Figure S5).

in the low micromolar range, for the full-length ERβ LBD and the ER 21-mer peptides. The binding affinities of the peptides showed only modest differences between the ER subtypes, in line with their highly similar amino acid sequences (Table 1). The overall affinities of the phosphorylated ER sequences were approximately 1 order of magnitude weaker than that of the SH2 high-affinity binding peptide **6**.[39] These binding affinities most probably result from variations in the amino acid sequence immediately C-terminal of the phosphotyrosine, as shown before for other Src target sequences,[40−43] and bring forward an archetypal affinity regime for SH2 binding by the phosphorylated ER constructs.

In order to identify the minimal ER binding motif, an FP based competition assay with pERα and pERβ peptides of different lengths was performed. Nonphosphorylated ERα/β sequences were each time included but did not exhibit any

DOI: 10.1021/acschembio.5b00568
ACS Chem. Biol. 2015, 10, 2624−2632

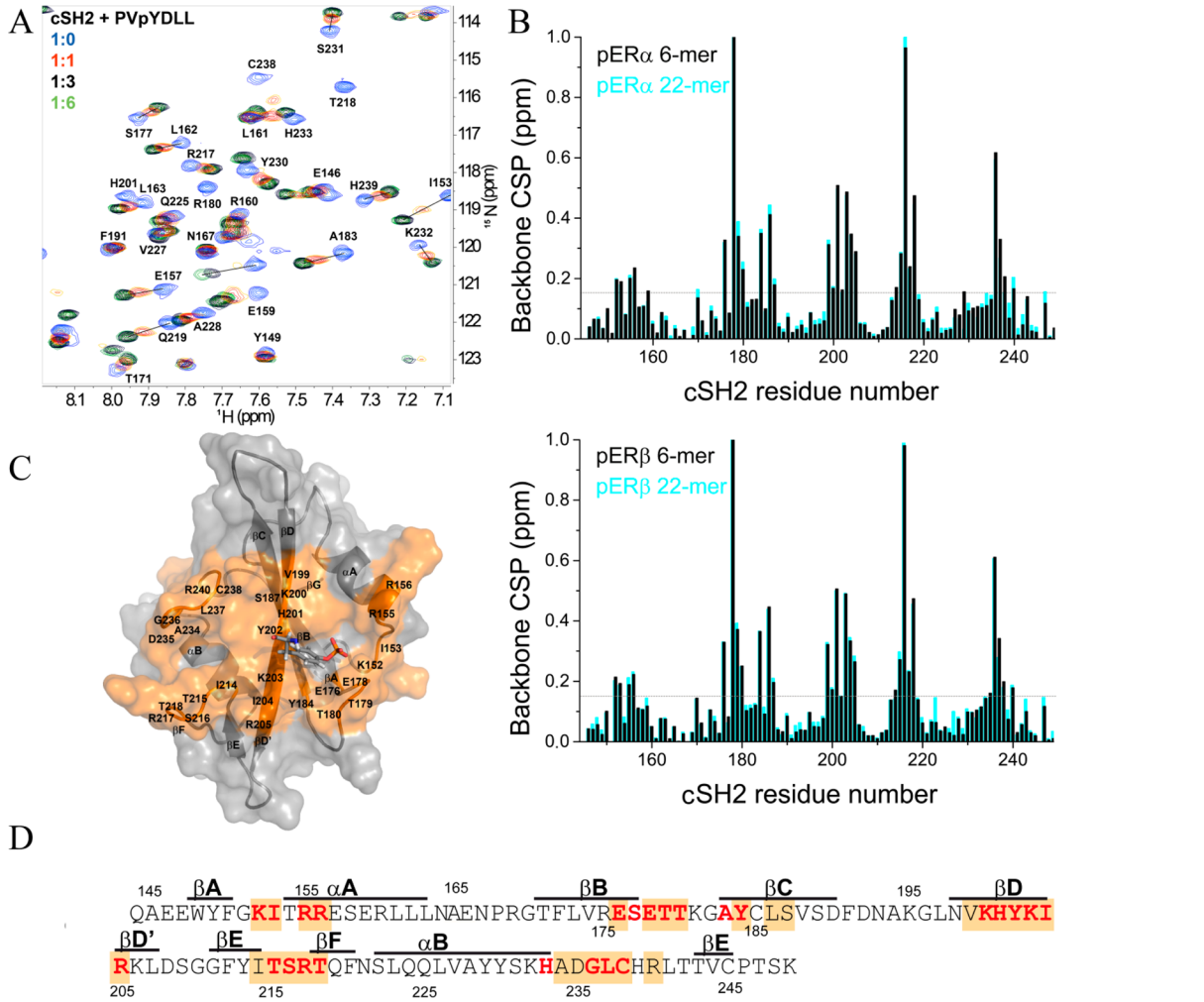

Figure 2. Characterization of the phosphorylated ER binding site on cSrc kinase SH2 domain (cSrc SH2). (A) Superimposition of a zoomed area from the ^{15}N-HSQC spectra of ^{15}N-cSrc SH2 in the presence of increasing amounts of the pERβ 6-mer peptide (PVpYDLL), at 1:0 (blue), 1:1 (red), 1:3 (black), and 1:6 (green) protein/peptide ratios. (B) Backbone chemical shift perturbations (CSP) of cSrc SH2 in complex with peptides pERα 6-mer (top, black), pERα 22-mer (top, cyan), pERβ 6-mer (bottom, black), and pERβ 22-mer (bottom, cyan). (C) Residues significantly perturbed (with a cutoff value CSP $\geq$ 0.15 ppm) upon ER binding are highlighted in orange on the cSrc SH2 structure[47] (PBD file 1HCS). (D) Sequence of the cSrc SH2 domain secondary structure elements. Residues significantly perturbed upon ER binding (as in C) are shaded in orange. For comparison, residues significantly perturbed upon GpYEEI binding (with a cutoff value CSP $\geq$ 0.15 ppm) are colored red.

detectable binding affinity to the Src SH2 domains. Moreover, any substitution of the phosphotyrosine of interest for either phosphoserine or glutamic acid as a negatively charged analog resulted to be detrimental for SH2 binding (Figure S7A,B). This is in line with previous results that indicate that the SH2 phosphotyrosine (pY) pocket is tightly structured and hence not adaptable to other amino acids.[44] IC_{50} values in the micromolar range were typically observed for all the relevant phosphorylated ER peptides (Table S2). Shortening the phosphorylated peptide length to 6-mers did typically not affect the binding affinity strongly. To pinpoint the minimal binding sequence, specific N- and C-terminal truncations were made based on the ERα 6-mer $_{535}$PLpYDLL$_{540}$ sequence (Figure S7C, Table S3). Compared to this motif, the C-terminal truncated peptide $_{534}$VPLpYD$_{538}$ featured a 3-fold weaker IC_{50}, indicating that the two leucines at the +2 and +3 positions of the phosphotyrosine are involved in the peptide binding to SH2. Further C-terminal truncation of the aspartic acid, resulting in peptide $_{533}$VVPLpY$_{537}$, yielded a 12-fold weaker IC_{50}. These results bring forward the important role of the previously described ionic interaction via the negatively charged amino acid side chain in the +1 position with respect to the phosphotyrosine.[45] For the phosphorylated ER sequence, this ionic interaction increases the affinity approximately 10-fold, which is in line with results from MD simulations (*vide infra*).

Mapping the SH2-ER Binding Site by NMR. ^{1}H−^{15}N-HSQC titrations[46] were performed to monitor local changes in cSrc SH2 protein structure upon binding of phosphorylated ERα/β peptide sequences of different lengths and the phosphorylated complete ERβ LBD. The observed chemical shift perturbations (CSP) provide a qualitative analysis of the resulting structural effects. The cSrc kinase SH2 domain was ^{15}N-enriched, and the assignment of its ^{1}H and ^{15}N resonances (Figure S8) was based on those reported earlier by Xu et al.[47] As an example for the SH2-pER binding studies, the short pERβ 6-mer peptide (PVpYDLL) was titrated to a solution of ^{15}N-enriched cSrc kinase SH2 domain, and ^{1}H−^{15}N-HSQC experiments were collected at four protein/peptide ratios, namely 1:0, 1:1, 1:3, and 1:6 (Figure 2A). The addition of the

DOI: 10.1021/acschembio.5b00568
ACS Chem. Biol. 2015, 10, 2624−2632

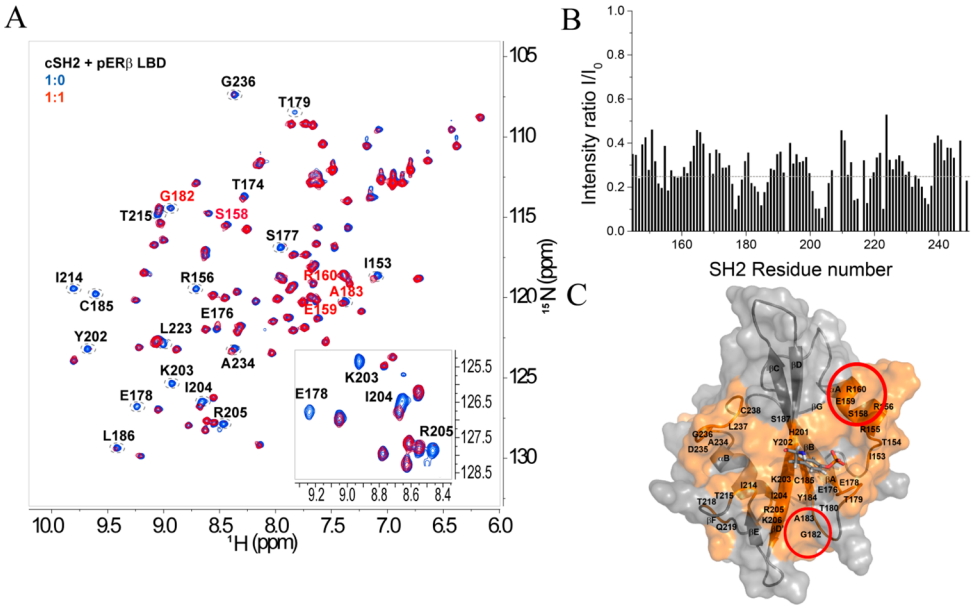

Figure 3. Characterization of the interaction of the phosphorylated ER LBD with the cSrc kinase SH2 domain. (A) Superimposition of a zoomed area from the ^{15}N-HSQC spectra of ^{15}N-cSrc SH2 in the absence (blue) and in the presence (1:1) of pERβ LBD (red). Residue peaks significantly affected upon the addition of pERβ LBD are highlighted with dotted circles. (B) Fractional changes in resonance intensities (I/I_0) observed for cSrc SH2 resonances in complex with 1:1 pERβ LBD. Note that a value of zero indicates that the resonance associated is no longer apparent or not measurable. The peaks corresponding to residues N193, S216, and S248 were not detected at pH 7.5 and were thus included with a value of zero in this graph. (C) Residues significantly perturbed upon ER LBD domain binding (with a cutoff value $I/I_0 < 0.25$) are highlighted in orange on the cSrc SH2 structure[47] (PBD 1HCS). Residues of additional extended recognition regions by the entire LBD, when compared to the titrations of the ER peptides, are highlighted in a red circle. Residue Q219 is affected in all titrations, but only slightly above the threshold for the titration of the ER entire LBD.

peptide resulted in strong and clear chemical shift changes in the HSQC spectra. No further chemical shift changes were observed beyond the 1:3 titration point, indicating binding saturation. Spectra for other cSrc SH2-pERα/β complexes were therefore subsequently recorded with a 6-fold molar excess of the phosphorylated peptide to ensure saturation of complex formation. The SH2 chemical shift changes upon addition of the phosphorylated peptides were as a whole rather similar (Figures 2B and S9). No differences (CSPs $\geq$ 0.05 ppm) were observed when comparing the ERα and ERβ subtypes for peptides of the same length. This shows, as observed with the fluorescence data, that the ER−SH2 interaction has no specific ER subtype preference, in line with the very similar peptide sequences of the ERα and ERβ around the phosphorylated tyrosine. Relevant differences (CSPs $\geq$ 0.05 ppm) did come forward when comparing ER peptides of different lengths (6-mer versus 22-mer)

The SH2 residues strongly affected in the titrations with the four different ER peptides (CSP $\geq$ 0.15 ppm) were summed up in a model (highlighted in orange in Figure 2C). Some of the most pronounced CSPs were observed for SH2 residues located at the core of its central β-sheet structure. These residues, located in the more rigid SH2 secondary structure regions, correspond to E176 (βB strand), Y184 and L186 (βC strand), V199 and H201−I204 (βD strand), R205 (βD′ strand), and T218 (βF strand). Overall, these spectral changes can be explained by binding of the phosphopeptides to the canonical phosphorylation recognition site of the SH2 domain. In addition, residues E178−T180 in the BC loop, residues T215−R217 in the EF loop, and residues A234−R240 in the BG loop experienced large chemical-shift changes upon pER binding. Particularly, residues E178 and S216, located in BC and EF loops, respectively, showed the two highest CSP values identified (above 1 ppm). Residue E178 is located in the vicinity (<3 Å) of the ER phosphotyrosine, whereas residue S216 is close to the C-terminal side of the peptide binding motif: the Leu+3 side chain of pYDLL in the ERα/β sequences. As reported earlier for other phosphopeptides,[48] our data indicate that binding of ER peptides to the cSrc SH2 domain could involve the ordering of the BG loop and a movement of the EF loop away from the BG loop, to accommodate the binding of the +3 position leucine and adjacent residues.

A more detailed analysis of the CSPs revealed specific differences (CSPs $\geq$ 0.05 ppm) between the titrations of the pER peptides of different lengths (Figure 2B). Residues I214 (βE4) and L237 (BG4) were more affected in the titration with the 6-mer peptides (black) than with the 22-mer peptides (cyan). According to the available crystal structure of the SH2−pYEEI complex,[45] these SH2 residues are in close proximity to each other and are involved in direct interactions with the +2 and +3 positions with respect to the phosphotyrosine of interest. SH2 residues L223 and V227, located in the αB helix, were more affected in the titration of the ERβ 22-mer peptide compared to the ERβ 6-mer peptide. Other residues of the BG loop, such as H239, R240, T242, and T243, also shifted more upon the addition of the long peptides. These residues are in the vicinity of G236 and L237, key residues in mediating peptide binding at the +3 site, and thus providing an indication for direct and/or indirect contacts beyond the minimal binding motif. The segment C-terminal to the phosphorylated tyrosine, including the leucines at the +2 and +3 positions, constitutes the helix 12 of the ER LBD. Phosphorylation of the tyrosine has been shown to have a structuring effect on helix 12,[9]

DOI: 10.1021/acschembio.5b00568
ACS Chem. Biol. 2015, 10, 2624−2632

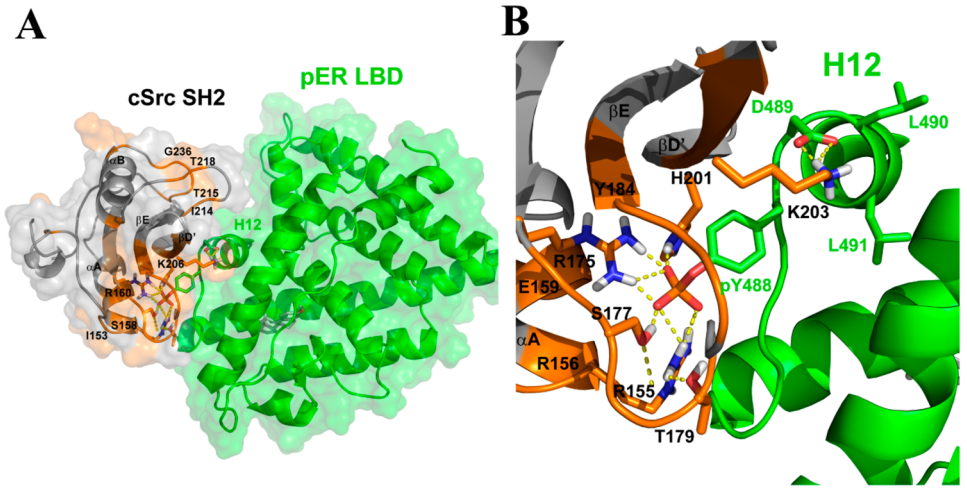

Figure 4. 3D model of the pERβ LBD−cSrc SH2 complex. The SH2 domain is shown in gray and ERβ LBD in green. SH2 residues significantly perturbed in the NMR titration with the ER LBD are highlighted in orange. (A) Full view of the complex, including a surface representation. (B) Close-up of the conserved interactions of the ER phosphotyrosine with cSrc SH2 residues and the helical organization of the amino acids C-terminal to the pY488, located in helix 12 (H12). Because of the H12 folding, the aspartic acid (D489) is well positioned to undergo ionic interactions with the SH2 lysine (K203). ER leucines L490 and especially L491 are oriented away from the SH2 domain and not available for interactions via the "Two-Pronged Plug Two-Holed Socket."

providing a first explanation for these peptide length dependent observations (*vide infra*).

Comparison of ER Motif and Consensus Sequence. A general comparison of the pER sequence titrations with a titration of the consensus peptide GpYEEI (Figures 2D and S10) showed that the cSrc SH2 domain generally uses similar interactions to mediate binding to these two types of peptides. A more detailed analysis of the CSPs, however, reveals interesting differences between the titrations of the pER 6-mer peptides and the GpYEEI peptide, resulting from interactions of the different residues in the epitope binding sequence (Figure S10C). On one hand, cSrc SH2 residues T179 (loop BC), L186 (βC), and V199 (βD) experienced larger perturbations (CSP > 0.2 ppm) upon the addition of the phosphorylated ER sequences compared to the GpYEEI titration. In the original crystal structure of the 11-mer -GpYEEI-peptide-Src SH2 complex,[45] T179 (loop BC) and L186 (βC) are in close vicinity to the pY side chain. On the other hand, cSrc SH2 residue Y202 (βD5) showed clearly a higher CSP value (CSP > 0.2 ppm) in the case of the GpYEEI titration. In the aforementioned crystal structure, Y202 (βD5) appears to play a key role in the interaction with SH2, by forming a portion of the Ile+3 binding cavity and specifically interacting with the Ile+3 side chain. Also this residue has direct contact with the Glu+1 side chain of the pYEEI peptide. Asp+1 in the ER sequences, in contrast, interacts through electrostatic interactions with H201 (βD4) and K203 (βD6) on the surface of the SH2 domain (*vide infra* MD simulations). In the ER sequence, the replacement of Glu+1 by Asp+1 and Ile+3 by Leu+3 may lead, according to the obtained CSPs, to weaker interactions with Y202 (βD5). This observation provides for a molecular explanation of the around 10-fold lower SH2 binding affinities obtained for the pER peptides, compared to the GpYEEI peptide.

Full-length pERβ LBD Binding to cSrc SH2. We have previously developed a protein semisynthesis approach to generate tyrosine-phosphorylated ER LBDs, and this strategy allowed, for the first time, crystallization of a PTM-containing ER LBD.[35] For the current work, a series of cocrystallization studies with the full length tyrosine-phosphorylated ER LBD and cSrc SH2 domain were attempted. Unfortunately, this did not lead to well diffracting protein crystals. Therefore, the molecular characteristics of the interaction of the full length tyrosine-phosphorylated ERβ LBD with the cSrc SH2 domain were elucidated by NMR. Titration of the ∼30 kDa phosphorylated ERβ LBD to the cSrc SH2 domain resulted in significant effects on the signal intensities of the SH2 domain (Figure 3A,B). These observations suggest the SH2 resonances to be in intermediate chemical exchange. Especially, residues S177 and E178 (βB) and Y202 (βD5)-R205 (βD′1) became almost undetectable (see also inset in Figure 3A). Also, a significant intensity decrease was observed for residues R156 (αA), E176 (βB), T179 (BC), Y184, L186−S187 (βC), H201 (βD), K206 (βD′), I214 (βE4), T215 (EF1), T218−Q219 (βF), and L223 and A234−C238 (βG4) (Figure 3). The resonances affected by line broadening were coherent with those featuring chemical shift changes in the experiments carried out with the phosphorylated ER peptides. Beyond this molecular regime, also the SH2 residues G182, A183, C185 (βC) and S158, E159, and R160 (αA) were affected upon titration of pERβ LBD (Figure 3). This observation hints to an additional extended recognition region upon ER LBD binding, comprising certain residues of the βC sheet and αA helix of the SH2 domain. The full length ER LBD thus addresses similar SH2 amino acids as the ER peptide but also provides additional contacts.

MD- and NMR-based 3D Model of ER-SH2 Complex. Based on the NMR titration data, a 3D model of the pERβ−cSrc SH2 complex was formulated by molecular dynamics (MD) simulations. The complex of the ERβ subtype with cSrc SH2 was pursued since the crystal structure of the phosphorylated ERβ LBD protein is available.[35] Initial coordinates were obtained by superposition of the phosphorylated ER peptide ($_{486}$PVpYDLL$_{491}$; see the Methods Section) or the pERβ LBD protein (PDB 3OLL), with the phosphotyrosine as a reference, into the NMR coordinates of the binary pYEEI−cSrc SH2 complex[47] (PDB 1HCS). This assumption was based on the high similarities of SH2 residues binding to

DOI: 10.1021/acschembio.5b00568
ACS Chem. Biol. 2015, 10, 2624−2632

the phosphorytosine affected in the titrations with the ER and pYEEI peptides. During 5 ns MD simulations, the overall binding orientation and dynamics of the complexes were maintained and the ER contacts with the SH2 domain were optimized (Figures S11 and S12). Interestingly, and in contrast to the known X-ray structure of the pYEEI−cSrc SH2 complex,[45] the SH2-bound pERβ peptide was found in both a partially extended and a helical conformation along the MD simulation. The leucine at the pTyr+2 position showed a preferred helical conformation at about 70% of the simulation, whereas the leucine at the pTyr+3 position showed a preferred extended conformation at about 60% of the simulation. This dual conformation can be seen in the ϕ/ψ distributions for the two leucine residues +2 and +3 from the phosphorylated tyrosine in Figure S13. Sequences that bind to SH2 in a partially helical conformation have been reported before and have been directly correlated with the nature of the residue at position pTyr+3.[49] In the MD simulations, the segment of residues pTyr−1 to +1 ($_{487}$VpYD$_{489}$) showed a stable extended conformation (Figure S13) and resembles well the ϕ/ψ values of the initial NMR coordinates from the pYEEI−cSrc SH2 complex (PDB 1HCS;[47] Table S4). During the simulation, the 6-mer pERβ peptide was able to make stable contacts with the tightly structured pY pocket of the SH2 domain, for instance, between the phosphate of the pTyr and SH2 residues R175 (βB5), S177, and T179 (Table S5). In contrast, the pTyr+3 binding pocket was clearly less defined in the SH2 structures during the simulation. The ER Leu+3 was located far from the hydrophobic cavity that is present in the "two-pronged" model of binding. The observation of the deviation from the two-pronged model as a result of ER binding indicates that our SH2 structure is more similar to the apo SH2 NMR structure,[44] upon ER binding, showing a shallower, weaker, second binding pocket. These observations further demonstrate the ability of the SH2 domain to accommodate diverse ligands, via conformational adaptation.[44]

For the full length LBD, residues pTyr+1, + 2, and +3 ($_{489}$DLL$_{491}$) are actually part of the LBD helix 12 (Figure 4B). In previous CD spectroscopy and structural studies in the absence of SH2, we have observed the intrinsically helical secondary structure of the H12 region of ER LBD, whose length can be regulated by phosphorylation of the key tyrosine residue.[9] In both phosphorylated and nonphosphorylated states, the here disclosed SH2 binding motif was found to be helical. The leucine amino acids, located at the pTyr+2 and +3 positions (pYDLL), are strong helix formers, whereas the tyrosine acts as a helix initiator upon phosphorylation, as also visible in the crystal structure of the pERβ LBD.[35] In the binding model of the pERβ LBD−SH2 complex, the ϕ/ψ distributions showed a defined conformational space along the MD simulation for the dihedral angles of the ER epitope $_{486}$PVpYDLL$_{491}$, well resembling the initial coordinates for the ER LBD structure (3OLL, Table S4). During the 5 ns MD simulation of the SH2 bound to the complete pERβ LBD protein, the leucine amino acids located at the pTyr+2 and +3 positions were found solely in a helical conformation. The analysis of the intermolecular hydrogen bonds showed several hydrogen bonds conserved throughout the simulation time. For instance, the phosphate group of the ER phosphotyrosine was kept salt-bridged to the SH2-conserved R175 (βB5), with an occupancy of 97% during the simulation. Other hydrogen bonds found involving pTyr were with S177 (72%), H201 (57%), R155 (27%), and T179 (19%). It is worth noting that not all these key interacting residues showed important variations in the HSQC experiments. This can be explained by the earlier proposition that the primary pTyr pocket is largely predefined before binding, with the structure and dynamics unchanged upon SH2 partner binding.[44]

The ER LBD Asp+1 showed transient salt-bridges with basic residues H201 (28%) and K203 (40%) on the SH2 surface. In the 3D model of the complex shown in Figure 4B, Asp+1 is making interactions that explain the importance of Asp+1 in the binding to SH2, as observed during the binding studies. As observed for the ERβ peptide, also for the full length LBD the Leu+3 is located far from the hydrophobic cavity that would support the "two-pronged" model binding. A comparison of the binding mode of the pYEEI consensus sequence with that of the corresponding pERβ sequence reveals the different orientation between both sequences of the amino acids C-terminal of the phosphorylated tyrosine (Figure S14). The pYEEI sequence features an extended conformation with the isoleucine (I+3) addressing the hydrophobic cavity that is present in the "two-pronged" model of binding. For the pERβ LBD, the aspartic acid (D+1) and two leucines (L+2 and L+3) are in a helical conformation with their side-chains repositioned and not addressing the hydrophobic cavity present in the "two-pronged" binding model. Because of this helical orientation, the Leu3+ residue does not play a key role in determining the binding affinity of the full ER to cSrc SH2, as also supported by the binding data. The interaction of the ER LBD with the cSrc SH2 domain is, thus, not surprisingly, primarily dictated by the phosphotyrosine binding to the SH2 binding site. The ER LBD, and specifically the AF2 domain, subsequently modulates the binding of the surrounding amino acids and tunes the interaction strength via the folding into a novel helical SH2 binding mode.

Conclusions. The first molecular insights in a protein−protein interaction relevant for nongenomic estrogen receptor signaling were obtained in a chemical biology approach, rooted in well-defined semisynthetic protein constructs and a combined biochemical and structural biology approach. The estrogen receptor−cSrc kinase interaction could be characterized, and a 3D model of the pERβ LBD−SH2 complex was obtained, culminating in the elucidation of a novel binding modus, strongly modulated by the folding of the ER helix 12. This mode of interaction constitutes a remarkable difference from the classical mode of binding in the archetypal pYEEI−cSrc SH2 complex.[45]

The short ERα and ERβ peptide motifs $_{535}$PLpYDLL$_{540}$ and $_{486}$PVpYDLL$_{491}$ encompass the minimal binding epitope for binding to SH2. The central phosphotyrosine is, expectedly, of absolute necessity for the interaction and binds to the Src SH2 domain via its canonical phosphorylation recognition site. The C-terminal leucines in the ER peptides address the second SH2 binding site in a partially helical conformation. Within the full length ER LBD, the phosphotyrosine binding motif is folded but functionally available for binding to cSrc SH2. The folding of the ER helix 12 provides for previously unrecognized binding interactions between the two proteins. Especially the C-terminal amino acids flanking the phosphotyrosine convey an ER specific interaction modus to the SH2 domain. The aspartate and two leucines at position pTyr+1, +2, and +3 are helical in the model, in agreement with the ER LBD helix 12-fold. As a result, especially the two leucines adopt a position away from the second, hydrophobic, SH2 cavity that would support the so-called classical "two-pronged" model binding.[45]

DOI: 10.1021/acschembio.5b00568
ACS Chem. Biol. 2015, 10, 2624−2632

The binding of the ER to this so-called specificity determining region of SH2 thus results from an interplay between SH2 plasticity and ER-determined protein folding.

The novel binding modus demonstrates the ability of the SH2 domain to accommodate sequences that bind in the secondary SH2 binding site with a largely dynamic conformation. This also highlights the difficulty of targeting SH2 domains for pharmaceutical purposes. Additionally, mutations around the ER phosphotyrosine, such as those reported to occur in breast cancer,[24−27] might further modulate the ER−cSrc interaction, resulting in a misregulation of both the genomic and nongenomic ER mediated signaling. The novel molecular approach reported here now provides an entry for the molecular elucidation of such events, potentially allowing for targeting the corresponding disease states.

METHODS

Protein Expression and Purification of Src SH2 Domains. Expression and purification of the cSrc and vSrc SH2 domains were performed as previously described,[50] with a few adjustments of the protocol, including cell lysis by using ice-water-cooled homogenization (EmulsiFlex C3, Avestin) in the presence of 5 mM DTT, 200 μM PMSF, and 1 μg mL^{-1} DNase.

The plasmid pET-3a_cSrcSH2 was transformed into *E. coli* BL21(DE) cells and grown overnight at 37 °C in 25 mL of LB medium precultures, containing 100 μg mL^{-1} ampicillin. Transfected expression cells were diluted in 2 L of rich TB medium in the presence of 100 μg mL^{-1} ampicillin at 37 °C. At an optical density of $OD_{600\ nm}$ ∼ 0.9, cells were pelleted (centrifugation at 6000 rpm for 10 min at 4 °C) and resuspended in 1 L of M9 minimal medium followed by the induction of protein expression by the addition of IPTG at a final concentration of 0.5 mM. Cells were incubated at 37 °C and 220 rpm overnight for protein expression, harvested by centrifugation at 7500 rpm and 4 °C, snap-frozen in N_2 (l), and stored at −80 °C until protein purification. Clarified and filtered cell extract was passed through two coupled 5 mL HiTrap SP FF columns (GE Healthcare) using an automated FPLC system (AKTA purifier). After washing off unbound protein, target protein was eluted with a gradient from 0 to 0.5 M NaCl in 20 mM Hepes at pH 7.5, 5 mM EDTA, and 5 mM DTT. The protein eluted at a salt concentration of about 0.2 M. Protein peak fractions were pooled and concentrated by Amicon Ultra 3K centrifugal filter devices, snap-frozen in aliquots, and stored at −80 °C in the elution buffer conditions.

ERα and ERβ LBD Protein Semisynthesis. The protein semisynthesis was performed as previously described.[9,35]

Fluorescence Polarization (FP) Direct Binding and Competition Assays. All peptides were dissolved in the buffer at pH 7.4 (50 mM Tris at pH 7.4, 150 mM NaCl, 10 mM $MgCl_2$, 0.05% (v/v) Tween-20, 0.5 mg mL^{-1} BSA, 1 mM TCEP). FAM-peptide assay concentrations were kept constant at 50 nM, and SH2 domains were serially diluted from high micromolar to low nanomolar concentration ranges. Fluorescence polarization was measured with a Tecan Safire monochromator microplate reader. Fluorescence polarization was determined by recording the excitation at 470 nm and emission at 519 nm. In the direct FP assay, the polarization ($[mP]$, Y) was plotted against the protein concentration ($[\log M]$, X). The resulting binding curves of the direct interaction assays were analyzed by formula 1, yielding the K_D values for the interactions.

$$Y = \mathrm{Bmax} \times X/(K_D + X) + \mathrm{BG} \quad (1)$$

with the maximum binding at saturating titrant concentrations (Bmax) and the background binding at low concentrations of titrant (BG).

In the FP competition assay, the fluorescent probe was kept constant at 20−25 nM and SH2 domain at 4−10 μM in 50 mM Tris-HCl at pH 7.5 with 100 mM NaCl and 2 mM DTT. The binding curves of the competition experiments were analyzed with formula 2, yielding the IC_{50} values for the competition by the individual peptide sequences.

$$Y = P_{\mathrm{bottom}} + (P_{\mathrm{top}} - P_{BOTTOM})/(1 + 10 \wedge ((X - \log \mathrm{IC}_{50}))) \quad (2)$$

with the top and bottom plateau (P).

NMR Spectroscopy. All NMR experiments were acquired at 298 K on a Bruker 750 or 900 MHz spectrometer. Unless otherwise stated, NMR samples of the ^{15}N-cSrc SH2 domain were prepared in MES buffer (pH 6.0) to a final concentration of 150 μM, containing 10% (v/v) D_2O. ^{1}H−^{15}N HSQC (heteronuclear single quantum correlation) spectra were acquired with 1024 complex data points in the ^{1}H dimension and 256 increments in the indirect dimension. For full details, see the Supporting Information.

Mapping the Interaction Surface. Backbone amide HSQC cross-peaks of the cSrc SH2 domain were monitored for each titration point of every experiment with each binding partner. A composite chemical shift change ($\Delta\delta_{av}$) for each residue was calculated as the weighted sum of the ^{1}H ($\Delta\delta_{HN}$) and ^{15}N ($\Delta\delta_N$) chemical shift changes as given in formula 3.

$$\Delta\delta_{av} = \{[(\Delta\delta_{HN})^2 + (\Delta\delta_N/5)^2]\}^{1/2} \quad (3)$$

Notation of cSrc SH2 secondary structure elements and residues was done according to the nomenclature of Waksman et al.[45]

Molecular Dynamic Simulations. MD simulations of three different pER−SH2 complexes were performed using an explicit solvent environment and the ff99SB force field[51] in the AMBER suite of programs[52] for (a) pERα 6-mer peptide-cSrc SH2, (b) pERβ 6-mer peptide-cSrc SH2, and (c) pERβ LBD-cSrc SH2. For full details, see the Supporting Information.

ASSOCIATED CONTENT

Supporting Information

The Supporting Information is available free of charge on the ACS Publications website at DOI: 10.1021/acschembio.5b00568.

Protocols and analytical data for protein expression and purification, protein semisynthesis, and peptide synthesis; experimental and supporting figures for fluorescence polarization assays; NMR; and molecular dynamics simulations (PDF)

AUTHOR INFORMATION

Corresponding Author

*E-mail: l.brunsveld@tue.nl.

Author Contributions

§These authors contributed equally to this work.

Funding

This work was supported by grants from Netherlands Organisation for Scientific Research via Gravity program 024.001.035, ECHO grant 711.011.017 and Large grant 175.107.301.10, and Marie Curie Actions to L.N. (PIEF-GA-561 2011−298489).

Notes

The authors declare no competing financial interest.

REFERENCES

(1) A Unified Nomenclature System for the Nuclear Receptor Superfamily. *Cell* 1999, *97*, 161−163.

(2) Brzozowski, A. M., Pike, A. C. W., Dauter, Z., Hubbard, R. E., Bonn, T., Engström, O., Öhman, L., Greene, G. L., Gustafsson, J.-Å., and Carlquist, M. (1997) Molecular basis of agonism and antagonism in the oestrogen receptor. *Nature 389*, 753−758.

(3) Nichols, M., Rientjes, J. M. J., and Stewart, A. F. (1998) Different positioning of the ligand-binding domain helix 12 and the F domain of the estrogen receptor accounts for functional differences between agonists and antagonists. *EMBO J. 17*, 765−773.

DOI: 10.1021/acschembio.5b00568
ACS Chem. Biol. 2015, 10, 2624−2632

(4) McKenna, N. J., Lanz, R. B., and O'Malley, B. W. (1999) Nuclear Receptor Coregulators: Cellular and Molecular Biology. *Endocr. Rev. 20*, 321−344.
(5) McKenna, N. J., and O'Malley, B. W. (2002) Combinatorial Control of Gene Expression by Nuclear Receptors and Coregulators. *Cell 108*, 465−474.
(6) Faus, H., and Haendler, B. (2006) Post-translational modifications of steroid receptors. *Biomed. Pharmacother. 60*, 520−528.
(7) Atsriku, C., Britton, D. J., Held, J. M., Schilling, B., Scott, G. K., Gibson, B. W., Benz, C. C., and Baldwin, M. A. (2009) Systematic Mapping of Posttranslational Modifications in Human Estrogen Receptor-α with Emphasis on Novel Phosphorylation Sites. *Mol. Cell. Proteomics 8*, 467−480.
(8) Le Romancer, M., Poulard, C., Cohen, P., Sentis, S., Renoir, J.-M., and Corbo, L. (2011) Cracking the Estrogen Receptor's Posttranslational Code in Breast Tumors. *Endocr. Rev. 32*, 597−622.
(9) Tharun, I. M., Nieto, L., Haase, C., Scheepstra, M., Balk, M., Möcklinghoff, S., Adriaens, W., Dames, S. A., and Brunsveld, L. (2015) Subtype-Specific Modulation of Estrogen Receptor−Coactivator Interaction by Phosphorylation. *ACS Chem. Biol. 10*, 475−484.
(10) Lösel, R., and Wehling, M. (2003) Nongenomic actions of steroid hormones. *Nat. Rev. Mol. Cell Biol. 4*, 46−55.
(11) Norman, A. W., Mizwicki, M. T., and Norman, D. P. G. (2004) Steroid-hormone rapid actions, membrane receptors and a conformational ensemble model. *Nat. Rev. Drug Discovery 3*, 27−41.
(12) Marino, M., Galluzzo, P., and Ascenzi, P. (2006) Estrogen Signaling Multiple Pathways to Impact Gene Transcription. *Curr. Genomics 7*, 497−508.
(13) Heldring, N., Pike, A., Andersson, S., Matthews, J., Cheng, G., Hartman, J., Tujague, M., Ström, A., Treuter, E., Warner, M., and Gustafsson, J.-Å. (2007) Estrogen Receptors: How Do They Signal and What Are Their Targets. *Physiol. Rev. 87*, 905−931.
(14) Barletta, F., Wong, C.-W., McNally, C., Komm, B. S., Katzenellenbogen, B., and Cheskis, B. J. (2004) Characterization of the Interactions of Estrogen Receptor and MNAR in the Activation of cSrc. *Mol. Endocrinol. 18*, 1096−1108.
(15) Cheskis, B. J., Greger, J., Cooch, N., McNally, C., Mclarney, S., Lam, H.-S., Rutledge, S., Mekonnen, B., Hauze, D., Nagpal, S., and Freedman, L. P. (2008) MNAR plays an important role in ERa activation of Src/MAPK and PI3K/Akt signaling pathways. *Steroids 73*, 901−905.
(16) Migliaccio, A., Castoria, G., Di Domenico, M., de Falco, A., Bilancio, A., Lombardi, M., Barone, M. V., Ametrano, D., Zannini, M. S., Abbondanza, C., and Auricchio, F. (2000) Steroid-induced androgen receptor−oestradiol receptor β−Src complex triggers prostate cancer cell proliferation. *EMBO J. 19*, 5406−5417.
(17) Auricchio, F., Migliaccio, A., and Castoria, G. (2008) Sex-steroid hormones and EGF signalling in breast and prostate cancer cells: Targeting the association of Src with steroid receptors. *Steroids 73*, 880−884.
(18) Varricchio, L., Migliaccio, A., Castoria, G., Yamaguchi, H., de Falco, A., di Domenico, M. D., Giovannelli, P., Farrar, W., Appella, E., and Auricchio, F. (2007) Inhibition of Estradiol Receptor/Src Association and Cell Growth by an Estradiol Receptor α Tyrosine-Phosphorylated Peptide. *Mol. Cancer Res. 5*, 1213−1221.
(19) Yudt, M. R., Vorojeikina, D., Zhong, L., Skafar, D. F., Sasson, S., Gasiewicz, T. A., and Notides, A. C. (1999) Function of Estrogen Receptor Tyrosine 537 in Hormone Binding, DNA Binding, and Transactivation. *Biochemistry 38*, 14146−14156.
(20) Weis, K. E., Ekena, K., Thomas, J. A., Lazennec, G., and Katzenellenbogen, B. S. (1996) Constitutively active human estrogen receptors containing amino acid substitutions for tyrosine 537 in the receptor protein. *Mol. Endocrinol. 10*, 1388−1398.
(21) Pietras, R. J., Arboleda, J., Reese, D. M., Wongvipat, N., Pegram, M. D., Ramos, L., Gorman, C. M., Parker, M. G., Sliwkowski, M. X., and Slamon, D. J. (1995) HER-2 tyrosine kinase pathway targets estrogen receptor and promotes hormone-independent growth in human breast cancer cells. *Oncogene 10*, 2435−2446.
(22) Tremblay, G. B., Tremblay, A., Labrie, F., and Giguère, V. (1998) Ligand-independent Activation of the Estrogen Receptors α and β by Mutations of a Conserved Tyrosine Can Be Abolished by Antiestrogens. *Cancer Res. 58*, 877−881.
(23) Skliris, G. P., Nugent, Z., Watson, P. H., and Murphy, L. C. (2010) Estrogen Receptor Alpha Phosphorylated at Tyrosine 537 is Associated with Poor Clinical Outcome in Breast Cancer Patients Treated with Tamoxifen. *Horm. Cancer 1*, 215−221.
(24) Toy, W., Shen, Y., Won, H., Green, B., Sakr, R. A., Will, M., Li, Z., Gala, K., Fanning, S., King, T. A., Hudis, C., Chen, D., Taran, T., Hortobagyi, G., Greene, G., Berger, M., Baselga, J., and Chandarlapaty, S. (2013) ESR1 ligand-binding domain mutations in hormone-resistant breast cancer. *Nat. Genet. 45*, 1439−1445.
(25) Robinson, D. R., Wu, Y.-M., Vats, P., Su, F., Lonigro, R. J., Cao, X., Kalyana-Sundaram, S., Wang, R., Ning, Y., Hodges, L., Gursky, A., Siddiqui, J., Tomlins, S. A., Roychowdhury, S., Pienta, K. J., Kim, S. Y., Roberts, J. S., Rae, J. M., Van Poznak, C. H., Hayes, D. F., Chugh, R., Kunju, L. P., Talpaz, M., Schott, A. F., and Chinnaiyan, A. M. (2013) Activating ESR1 mutations in hormone-resistant metastatic breast cancer. *Nat. Genet. 45*, 1446−1451.
(26) Li, S., Shen, D., Shao, J., Crowder, R., Liu, W., Prat, A., He, X., Liu, S., Hoog, J., Lu, C., Ding, L., Griffith, O. L., Miller, C., Larson, D., Fulton, R. S., Harrison, M., Mooney, T., McMichael, J. F., Luo, J., Tao, Y., Goncalves, R., Schlosberg, C., Hiken, J. F., Saied, L., Sanchez, C., Giuntoli, T., Bumb, C., Cooper, C., Kitchens, R. T., Lin, A., Phommaly, C., Davies, S. R., Zhang, J., Kavuri, M. S., McEachern, D., Dong, Y. Y., Ma, C., Pluard, T., Naughton, M., Bose, R., Suresh, R., McDowell, R., Michel, L., Aft, R., Gillanders, W., DeSchryver, K., Wilson, R. K., Wang, S., Mills, G. B., Gonzalez-Angulo, A., Edwards, J. R., Maher, C., Perou, C. M., Mardis, E. R., and Ellis, M. J. (2013) Endocrine-Therapy-Resistant ESR1 Variants Revealed by Genomic Characterization of Breast-Cancer-Derived Xenografts. *Cell Rep. 4*, 1116−1130.
(27) Jeselsohn, R., Yelensky, R., Buchwalter, G., Frampton, G., Meric-Bernstam, F., Gonzalez-Angulo, A. M., Ferrer-Lozano, J., Perez-Fidalgo, J. A., Cristofanilli, M., Gómez, H., Arteaga, C. L., Giltnane, J., Balko, J. M., Cronin, M. T., Jarosz, M., Sun, J., Hawryluk, M., Lipson, D., Otto, G., Ross, J. S., Dvir, A., Soussan-Gutman, L., Wolf, I., Rubinek, T., Gilmore, L., Schnitt, S., Come, S. E., Pusztai, L., Stephens, P., Brown, M., and Miller, V. A. (2014) Emergence of Constitutively Active Estrogen Receptor-α Mutations in Pretreated Advanced Estrogen Receptor−Positive Breast Cancer. *Clin. Cancer Res. 20*, 1757−1767.
(28) Zhang, Q.-X., Borg, Å., Wolf, D. M., Oesterreich, S., and Fuqua, S. A. W. (1997) An Estrogen Receptor Mutant with Strong Hormone-independent Activity from a Metastatic Breast Cancer. *Cancer Res. 57*, 1244−1249.
(29) Irby, R. B., and Yeatman, T. J. (2000) Role of Src expression and activation in human cancer. *Oncogene 19*, 5636−5642.
(30) Elsberger, B., Tan, B. A., Mallon, E. A., Brunton, V. G., and Edwards, J. (2010) Is there an association with phosphorylation and dephosphorylation of Src kinase at tyrosine 530 and breast cancer patient disease-specific survival. *Br. J. Cancer 103*, 1831−1834.
(31) Ishizawar, R., and Parsons, S. J. (2004) c-Src and cooperating partners in human cancer. *Cancer Cell 6*, 209−214.
(32) Sanchez, M., Picard, N., Sauvé, K., and Tremblay, A. (2010) Challenging estrogen receptor β with phosphorylation. *Trends Endocrinol. Metab. 21*, 104−110.
(33) Arnold, S. F., Obourn, J. D., Jaffe, H., and Notides, A. C. (1995) Phosphorylation of the human estrogen receptor on tyrosine 537 in vivo and by src family tyrosine kinases in vitro. *Mol. Endocrinol. 9*, 24−33.
(34) Sun, J., Zhou, W., Kaliappan, K., Nawaz, Z., and Slingerland, J. M. (2012) ERα Phosphorylation at Y537 by Src Triggers E6-AP-ERα Binding, ERα Ubiquitylation, Promoter Occupancy, and Target Gene Expression. *Mol. Endocrinol. 26*, 1567−1577.
(35) Möcklinghoff, S., Rose, R., Carraz, M., Visser, A., Ottmann, C., and Brunsveld, L. (2010) Synthesis and Crystal Structure of a

DOI: 10.1021/acschembio.5b00568
ACS Chem. Biol. 2015, 10, 2624−2632

Phosphorylated Estrogen Receptor Ligand Binding Domain. *ChemBioChem. 11*, 2251−2254.
(36) Phan, T., Nguyen, H. D., Göksel, H., Möcklinghoff, S., and Brunsveld, L. (2009) Phage display selection of miniprotein binders of the Estrogen Receptor. *Chem. Commun. 46*, 8207−8209.
(37) Zhou, S., Shoelson, S. E., Chaudhuri, M., Gish, G., Pawson, T., Haser, W. G., King, F., Roberts, T., Ratnofsky, S., Lechleider, R. J., Neel, B. G., Birge, R. B., Fajardo, J. E., Chou, M. M., Hanafusa, H., Schaffhausen, B., and Cantley, L. C. (1993) SH2 domains recognize specific phosphopeptide sequences. *Cell 72*, 767−778.
(38) Piccione, E., Case, R. D., Domchek, S. M., Hu, P., Chaudhuri, M., Backer, J. M., Schlessinger, J., and Shoelson, S. E. (1993) Phosphatidylinositol 3-kinase p85 SH2 domain specificity defined by direct phosphopeptide/SH2 domain binding. *Biochemistry 32*, 3197−3202.
(39) Pawson, T. (1995) Protein modules and signalling networks. *Nature 373*, 573−580.
(40) Ladbury, J. E., Lemmon, M. A., Zhou, M., Green, J., Botfield, M. C., and Schlessinger, J. (1995) Measurement of the binding of tyrosyl phosphopeptides to SH2 domains: a reappraisal. *Proc. Natl. Acad. Sci. U. S. A. 92*, 3199−3203.
(41) Bradshaw, J. M., Grucza, R. A., Ladbury, J. E., and Waksman, G. (1998) Probing the "Two-Pronged Plug Two-Holed Socket" Model for the Mechanism of Binding of the Src SH2 Domain to Phosphotyrosyl Peptides: A Thermodynamic Study. *Biochemistry 37*, 9083−9090.
(42) Bradshaw, J. M., and Waksman, G. (1999) Calorimetric Examination of High-Affinity Src SH2 Domain-Tyrosyl Phosphopeptide Binding: Dissection of the Phosphopeptide Sequence Specificity and Coupling Energetics. *Biochemistry 38*, 5147−5154.
(43) Charifson, P. S., Shewchuk, L. M., Rocque, W., Hummel, C. W., Jordan, S. R., Mohr, C., Pacofsky, G. J., Peel, M. R., Rodriguez, M., Sternbach, D. D., and Consler, T. G. (1997) Peptide Ligands of pp60c-src SH2 Domains: A Thermodynamic and Structural Study. *Biochemistry 36*, 6283−6293.
(44) Taylor, J. D., Ababou, A., Fawaz, R. R., Hobbs, C. J., Williams, M. A., and Ladbury, J. E. (2008) Structure, dynamics, and binding thermodynamics of the v-Src SH2 domain: Implications for drug design. *Proteins: Struct., Funct., Genet. 73*, 929−940.
(45) Waksman, G., Shoelson, S. E., Pant, N., Cowburn, D., and Kuriyan, J. (1993) Binding of a high affinity phosphotyrosyl peptide to the Src SH2 domain: Crystal structures of the complexed and peptide-free forms. *Cell 72*, 779−790.
(46) Farmer, B. T., Constantine, K. L., Goldfarb, V., Friedrichs, M. S., Wittekind, M., Yanchunas, J., Robertson, J. G., and Mueller, L. (1996) Localizing the NADP+ binding site on the MurB enzyme by NMR. *Nat. Struct. Biol. 3*, 995−997.
(47) Xu, R. X., Word, J. M., Davis, D. G., Rink, M. J., Willard, D. H., and Gampe, R. T. (1995) Solution structure of the human pp60c-src SH2 domain complexed with a phosphorylated tyrosine pentapeptide. *Biochemistry 34*, 2107−2121.
(48) Hu, J., and Hubbard, S. R. (2006) Structural Basis for Phosphotyrosine Recognition by the Src Homology-2 Domains of the Adapter Proteins SH2-B and APS. *J. Mol. Biol. 361*, 69−79.
(49) Nachman, J., Gish, G., Virag, C., Pawson, T., Pomès, R., and Pai, E. (2010) Conformational Determinants of Phosphotyrosine Peptides Complexed with the Src SH2 Domain. *PLoS One 5*, e11215.
(50) Waksman, G., Kominos, D., Robertson, S. C., Pant, N., Baltimore, D., Birge, R. B., Cowburn, D., Hanafusa, H., Mayer, B. J., Overduin, M., Resh, M. D., Rios, C. B., Silverman, L., and Kuriyan, J. (1992) Crystal structure of the phosphotyrosine recognition domain SH2 of v-src complexed with tyrosine-phosphorylated peptides. *Nature 358*, 646−653.
(51) Hornak, V., Abel, R., Okur, A., Strockbine, B., Roitberg, A., and Simmerling, C. (2006) Comparison of multiple Amber force fields and development of improved protein backbone parameters. *Proteins: Struct., Funct., Genet. 65*, 712−725.
(52) Case, D. A., Cheatham, T. E., Darden, T., Gohlke, H., Luo, R., Merz, K. M., Onufriev, A., Simmerling, C., Wang, B., and Woods, R. J. (2005) The Amber biomolecular simulation programs. *J. Comput. Chem. 26*, 1668−1688.

DOI: 10.1021/acschembio.5b00568
ACS Chem. Biol. 2015, 10, 2624−2632